Vol. 114: 229–237, 2015
doi: 10.3354/dao02868

DISEASES OF AQUATIC ORGANISMS
Dis Aquat Org

Published June 3

# Characterization of Chinese giant salamander iridovirus tissue tropism and inflammatory response after infection

**Nan Jiang[1,2], Yuding Fan[1], Yong Zhou[1], Wenzhi Liu[1], Jie Ma[1], Yan Meng[1], Congxin Xie[2], Lingbing Zeng[1,2,*]**

[1]Division of Fish Disease, Yangtze River Fisheries Research Institute, Chinese Academy of Fishery Sciences, Wuhan, Hubei 430223, PR China

[2]College of Fisheries, Huazhong Agricultural University, Wuhan, Hubei 430070, PR China

ABSTRACT: The Chinese giant salamander iridovirus (GSIV), belonging to the genus *Ranavirus* in the family *Iridoviridae*, causes severe hemorrhagic lesions and nearly 100% mortality in naturally infected Chinese giant salamanders *Andrias davidiamus*. However, the replication and distribution of the virus has not been well characterized *in vivo*. Using *in situ* hybridization, the expression of the GSIV major capsid protein (MCP) was detected in the cytoplasm of cells of the spleen, kidney, liver and gut tissues. MCP expression in the spleen and kidney appeared to fluctuate significantly during the acute phase of infection. Using an immunofluorescence assay, GSIV antigens were abundant in the spleen and kidney tissues but appeared to be at relatively low levels in the liver and gut. Additionally, there were significant changes in the expression of the pro-inflammatory cytokines macrophage migration inhibitory factor (MIF), tumor necrosis factor α (TNF-α) and interleukin-1β (IL-1β) in different tissues in response to infection with GSIV. The expression of MIF, TNF-α and IL-1β had significantly increased in the spleen at 3 d post-infection; this correlated with a decrease in virus replication in the spleen. These results suggest that the spleen and kidney are the major target tissues of GSIV, and the increased expression of MIF, TNF-α and IL-1β may contribute to a reduction of virus replication in the spleen.

KEY WORDS: Chinese giant salamander · Iridovirus · Replication · Tissue tropism · Inflammatory response



## INTRODUCTION

The Chinese giant salamander *Andrias davidianus* is one of the largest amphibian species in the world. The population of Chinese giant salamanders has decreased sharply due to infectious disease, habitat loss, environmental pollution and overharvesting (Wang et al. 2004). In the past few years, both juvenile and adult life stages of this animal have been impacted by various diseases. A disease caused by an iridovirus was recognized as the most severe for Chinese giant salamander (Dong et al. 2011, Geng et al. 2011, Jiang et al. 2011, Meng et al. 2014).

The Chinese giant salamander iridovirus (GSIV), belonging to the genus *Ranavirus* in the family *Iridoviridae*, was first reported in 2010 in Shanxi Province, and subsequently in Shaanxi, Sichuan, Jiangxi and Hubei Provinces. High mortality was reported in all cases (Dong et al. 2011, Geng et al. 2011, Jiang et al. 2011, Chen et al. 2013, Meng et al. 2014). The virus enters cells through endocytosis or fusion, replicates in the cytoplasm, and progeny viruses aggregate in pseudocrystalline arrays during the late phase of replication (Ma et al. 2014). Many organs, including the spleen, kidney and liver, are infected by GSIV, which leads to the development of clinical disease

*Corresponding author: zlb@yfi.ac.cn

(Cunningham et al. 2008, Balseiro et al. 2010, Robert et al. 2011). The major caspid protein (MCP) is the major structural component of iridovirus particles, accounting for up to 45% of all virus proteins (Tidona et al. 1998, Black et al. 1981, Hyatt et al. 2000). This protein is localized in areas of virus replication, and is required for the assembly and release of progeny virus. High levels of MCP expression correlate with a high yield of viral production (Zhao et al. 2007). Although GSIV has been investigated extensively, the modes of virus replication and distribution in different tissues *in vivo* during infection are still unknown.

The inflammatory response is a basic protective response to virus infection in vertebrates, but little is known about this response in amphibians. The macrophage migration inhibitory factor (MIF) inhibits the random migration of macrophages (Bernhagen et al. 1998) and functions as a pleiotropic protein that participates in both inflammatory and immune responses (Nishihira 2000). The MIF protein is mainly secreted by monocytes, macrophages and activated T-lymphocytes in response to immune and inflammatory stimuli (Calandra & Roger 2003). MIF can regulate extracellular regulated protein kinases 1 & 2 (ERK1/2) and trigger the expression of inflammatory cytokines, such as tumor necrosis factor (TNF) (Flaster et al. 2007). MIF also specifically counteracts the glucocorticoid-induced suppression of an inflammatory response (Calandra et al. 1995). MIF-deficient macrophages have lower innate cytokine production (Das et al. 2013) and lower pro-inflammatory function (Mitchell et al. 2002). Thus, MIF appears to be an indispensable mediator of the inflammatory response (Flaster et al. 2007). To date, very little is known about inflammatory responses in Chinese giant salamander. Recently, the Chinese giant salamander MIF gene sequence was identified, and its encoded protein was shown to have enzymatic redox and tautomerase activity, and was also capable of inhibiting the migration of macrophages (Wang et al. 2013). Ranavirus infection can up-regulate pro-inflammatory cytokines such as TNF-α and interleukin-1β (IL-1β) in fish and frogs (Morales et al. 2010, Holopainen et al. 2012), but the inflammatory responses to ranavirus infection have not been characterized in amphibian hosts, such as the Chinese giant salamander.

In the present study, to determine the replication and distribution of GSIV in the Chinese giant salamander and the relationship between the inflammatory response and GSIV infection, *in situ* hybridization was used to examine the expression pattern of MCP and an immunofluorescence assay was used to detect the virus antigen. Additionally, quantitative real-time PCR assays were used to measure the expression level of inflammation-related genes, including MIF, TNF-α and IL-1β *in vivo*.

## MATERIALS AND METHODS

### Animals, cells and virus

Apparently healthy 1 yr old Chinese giant salamanders were obtained from the Yangtze River Fisheries Research Institute, Chinese Academy of Fishery Sciences; these were kept in aerated tap water at 20 ± 2°C. GSIV was isolated from diseased Chinese giant salamanders and propagated in epithelioma papulosum cyprini (EPC) cells as previously described (Meng et al. 2014).

### Infection experiments and sample collections

A total of 64 Chinese giant salamanders were equally divided into a GSIV infection group and a mock-infection group injected with phosphate-buffered saline (PBS). In the GSIV infection group, each individual animal was injected intraperitoneally with 300 µl of a stock of GSIV that had a titer of $1 \times 10^7$ $TCID_{50}$ $ml^{-1}$ (50% tissue culture infective dose per milliliter). In the mock-infection group, each animal was injected intraperitoneally with 300 µl PBS (Sigma). At 3, 7, 12 and 15 d post-infection (dpi), the spleen, kidney, liver, gut, heart and skin were collected from 8 animals from each group. The tissues were fixed in either 4% paraformaldehyde (PFA) for sectioning or stored in TRIzol Reagent (Gibco Invitrogen) for RNA extraction.

### *In situ* hybridization

The primer used in the preparation of the digoxigenin (DIG)-labeled MCP probe was 5′-TCA CCA AGC TGC CGT CTC TG-3′; the reverse primer was 5′-GAG GTC CTG GAT GGC CCT CA-3′. The probe was synthesized using T7 RNA polymerase with a DIG RNA-labeling kit (Promega) following the manufacturer's procedures. PFA-fixed spleen, kidney, liver, gut, heart and skin were dehydrated with 30% sucrose/PBS and then embedded in optimum cutting temperature compound (OCT, Leica). Tissue

samples were sectioned (8 µm) at −20°C (UC7, Leica). The sections were rehydrated with PBS 3 times, and then the DIG-labeled MCP probe was added to the sections and incubated overnight at 65°C. The sections were incubated with anti-DIG antibody (1:4000; Roche Diagnostics), and then stained with NBT/BCIP (Roche Diagnostics) (Jiang et al. 2012). Sixty sections of each tissue were hybridized with the DIG-MCP probe and examined by light microscopy.

### Production of monoclonal antibody and immunofluorescence assay

The anti-GSIV mouse monoclonal antibody was produced by AN BIOTECH Co. Female BALB/c mice were immunized with the GSIV MCP protein in Freund's complete adjuvant (Sigma-Aldrich). Splenocytes from the immunized mice and SP2/0 myeloma cells were fused, positive hybrids were screened and subcloned 4 times. Monoclonal antibody was produced either from the supernatants of the hybridoma culture or from the ascites of BALB/c mice. Titers of the monoclonal antibody were determined by indirect ELISA. The specificity of monoclonal antibody was validated by Western blot.

EPC cells were either infected with GSIV at a multiplicity of infection of 0.1, or mock-inoculated with EMEM (Sigma). The infected cells were collected on Days 2 and 3 post-infection, and the mock-infected cells were collected on Day 3. The cells were homogenized in an ice-cold lysis buffer (Beyotime) containing protease-inhibitor (Roche Diagnostics) and sonicated for 3 s. The proteins in the cell homogenates were separated by SDS-PAGE and transferred to a 0.45 µm polyvinylidene fluoride membrane (Millipore). The membrane was blocked with Tris-buffered saline (TBS) containing 4% bovine serum albumin (BSA) and 5% fetal bovine serum (FBS) for 3 h, and then incubated with anti-GSIV mouse monoclonal antibody (1:1000) overnight. The membranes were washed with TBS and incubated with 1:10000 diluted horseradish peroxidase (HRP)-labeled goat anti-mouse Ig (Bio-Rad). The signal was detected by chemiluminescence (Bio-Rad).

Sections of spleen, kidney, liver, gut, heart and skin were rehydrated with PBS and blocked with 0.1% BSA/PBS for 3 h. Sections were incubated with anti-GSIV mouse monoclonal antibody (1:500) for 12 h at 4°C, washed with PBS, and then incubated with a 1:1000 dilution of Cy3-labeled goat anti-mouse (Beyotime). After washing, sections were counterstained with DAPI (1 µg $ml^{-1}$ in PBS) for 15 min. Sixty sections of each sample were examined and photographed using fluorescence microscopy.

### RT-PCR and quantitative real-time PCR

Total RNA from spleen, kidney, liver and gut were extracted with TRIzol Reagent according to the manufacturer's instructions. In order to eliminate the DNA, the samples were treated with DNase for 6 h and extracted by phenol/chloroform as previously described (Jiang et al. 2012). Reverse transcription of cDNA was performed according to the protocol of the ReverlAid First Stand cDNA Synthesis Kit (Thermo Scientific), with the following program: 65°C for 5 min, 4°C for 5 min, 42°C for 60 min and, finally, 70°C for 5 min. Real-time PCR was performed using the FastStart Universal SYBR Green Master (Roche Diagnostics). Each real-time PCR program included the following procedures: 95°C for 30 s, 95°C for 15 s, 60°C for 20 s and 72°C for 35 s; Steps 2–4 were repeated for 40 cycles. All primers used for real-time PCR are listed in Table 1. Chinese giant salamander 18S ribosomal RNA was

Table 1. Primers used in real-time PCR analysis. MIF: migration inhibitory factor; TNF-α: tumor necrosis factor α; IL-1β: interleukin-1β

| Target gene | Primer | Amplicon size (bp) | Accession no. or reference |
|---|---|---|---|
| MIF | Sense: 5′-CCAAATGATGTCCTTCGGT<br>Antisense: 5′-TCGGCTGGTATATGGAGTTC | 144 | JX041894 |
| TNF-α | Sense: 5′-ATGCCAGGACCAATGCTGGA<br>Antisense: 5′-GGCCAGGTGCCTGGTAAGAA | 91 | KM079078 |
| IL-1β | Sense: 5′-ACCTTCCGGAAGGCAGTGGT<br>Antisense: 5′-TTCTGCCATGGAGGTGACGT | 165 | KM103345 |
| 18S | Sense: 5′-CCTGAGAAACGGCTACCACATCC<br>Antisense: 5′-AGCAACTTTAGTATACGCTATTGGAG | | Yang et al. (2010) |

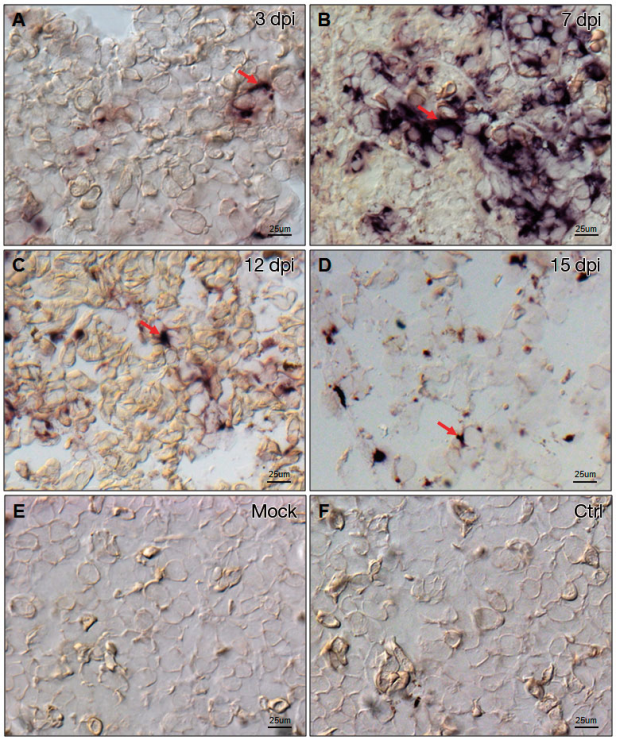


Fig. 1. *Andrias davidiamus*. *In situ* hybridization with a digoxigenin (DIG)-labeled RNA probe specific to the major capsid protein (MCP) in the spleen sections obtained from Chinese giant salamander iridovirus (GSIV)-infected salamanders. (A–D) Spleen sections sampled at 3, 7, 12 and 15 d post-infection (dpi). (E) Mock-infected spleen sections. (F) Ctrl: 15 dpi spleen stained with the secondary anti-DIG antibody alone. Arrows indicate a positive signal. Scale bars = 25 µm

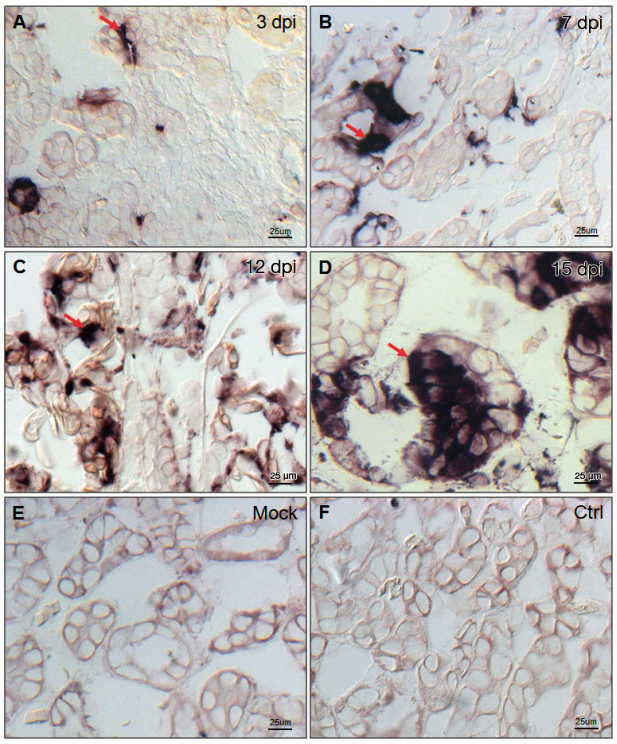


Fig. 2. *Andrias davidiamus*. As in Fig. 1 for kidney sections

used as an endogenous control to normalize the input of RNA samples (Yang et al. 2010).

### Statistical analysis

The number of positive cells and the total cells (>100 cells) in 5 areas of 1 section were counted. Twenty continuous sections of each tissue from 8 distinct animals were measured. The average percent positive cells ± the standard deviation (SD) for each tissue was determined. For the real-time PCR results, 3 replicates of each sample were expressed as means (±SD). The mRNA level of each gene in each sample was first calculated as the ratio with 18S ribosomal RNA transcript levels that were amplified as an internal control (Yang et al. 2010) and then expressed as a fold-increase relative to the mock infection groups. The data were analyzed by 1-way ANOVA followed by the Dunnett test. A $p \leq 0.05$ was considered to be significant. The results were repeated 3 times.

## RESULTS

### Expression patterns of the MCP gene

Temporal and spatial expression patterns of MCP in GSIV-infected Chinese giant salamanders were examined by *in situ* hybridization (Figs. 1–4). Positive signals were detected in the cytoplasm of cells in the spleen, kidney, liver and gut. In the spleen, the expression level of MCP peaked at 7 dpi and then decreased after 12 dpi (Fig. 1A–D). In the kidney, MCP signals increased over time and reached a peak at 15 dpi (Fig. 2A–D). Positive hybridizations were detected in the renal tubules, glomerulus and hematopoietic tissue. In the liver, MCP expression level did not increase significantly from 3 to 15 dpi (Fig. 3A–D). The MCP-positive signals in the mucosa epithelial cells and submucosa cells of the gut were detected at 7 dpi (Fig. 4A–D). No signal was detected in any tissue from the mock infection group (Figs. 1E, 2E, 3E & 4E). Additionally, no signal was detected at 15 dpi in any tissue from the infected groups when stained using only the anti-DIG antibody (Figs. 1F, 2F, 3F & 4F). In the heart and skin, no signal was observed for the infected or mock-infected groups (data not shown). The intensity of detection in each tissue is summarized in Table 2.

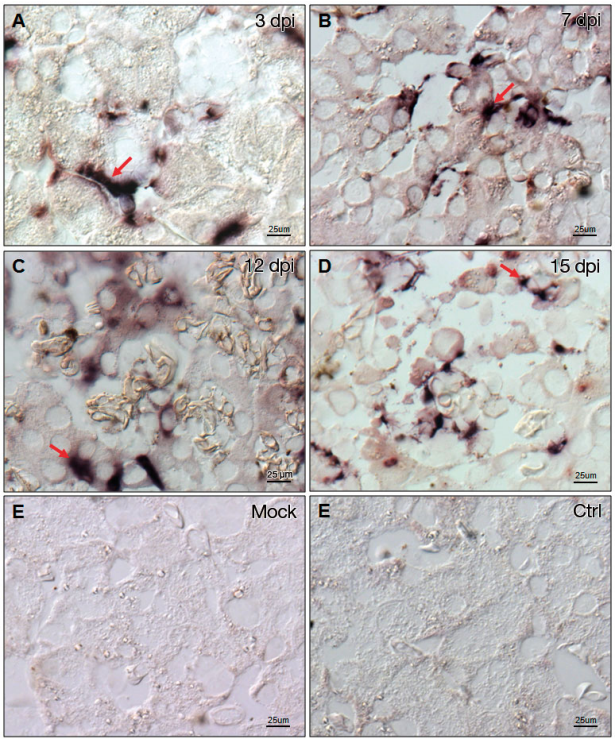


Fig. 3. *Andrias davidiamus*. As in Fig. 1 for liver sections

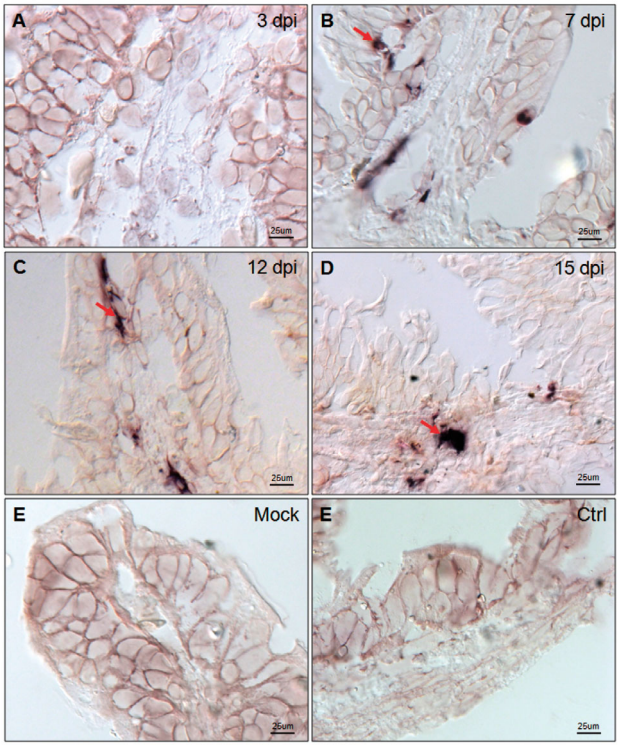


Fig. 4. *Andrias davidiamus*. As in Fig. 1 for gut sections

### Distribution of viral antigen

To determine the distribution of viral antigen, a monoclonal antibody specific to GSIV was used. Western blot was used to examine the specificity of the anti-GSIV monoclonal antibody. The monoclonal antibody reacted with the lysed homogenates of GSIV-infected EPC cells and recognized a band at 45 kDa. No band was observed in homogenates from mock-infected cells that reacted with the anti-GSIV monoclonal antibody (Fig. 5). By immunofluorescence assay (IFA), viral antigen was mainly detected in the cytoplasm (Figs. 6–9). In the spleen, the percentage of GSIV antigen-positive cells increased from 3 to 12 dpi, and then a high level was maintained (Fig. 6A–D). In the kidney, the GSIV antigen-positive cells increased over time, and reached a peak at 15 dpi. Positive signals were detected in the

Table 2. *Andrias davidiamus*. Mean (±SD) percentage of major capsid protein (MCP)-positive cells in tissue sections prepared from the spleen, kidney, liver and gut of Chinese giant salamanders that were experimentally infected with GSIV. The number of positive cells and total cells (>100 cells) in 5 areas of 1 section were counted; 20 continuous sections of each tissue from 8 animals were measured

| Days post-infection | Spleen (%) | Kidney (%) | Liver (%) | Gut (%) |
|---|---|---|---|---|
| 3 | 4.1 ± 0.3 | 5.8 ± 0.3 | 10.7 ± 0.2 | 0 |
| 7 | 66.3 ± 6.9 | 16.4 ± 2.4 | 18.1 ± 1.7 | 4.7 ± 0.4 |
| 12 | 22.5 ± 1.6 | 48.3 ± 4.2 | 19.4 ± 2.1 | 7.7 ± 1.0 |
| 15 | 20.5 ± 1.2 | 68.5 ± 6.4 | 17.4 ± 1.8 | 8.3 ± 1.2 |

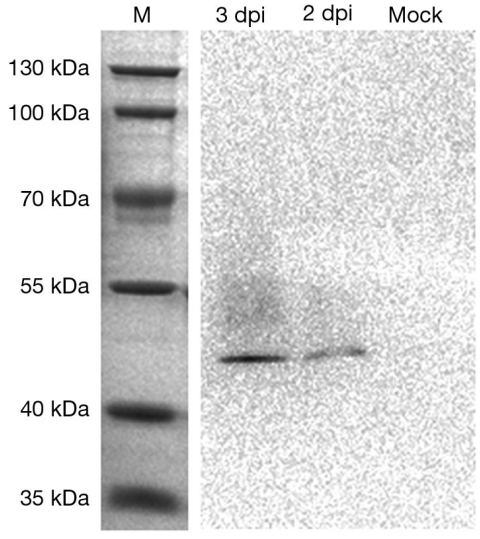


Fig. 5. Characterization of the specificity of anti-GSIV monoclonal antibody by Western blot. The homogenates of 2 and 3 dpi and mock-infected epithelioma papulosum cyprini were probed with anti-GSIV monoclonal antibody. M: marker

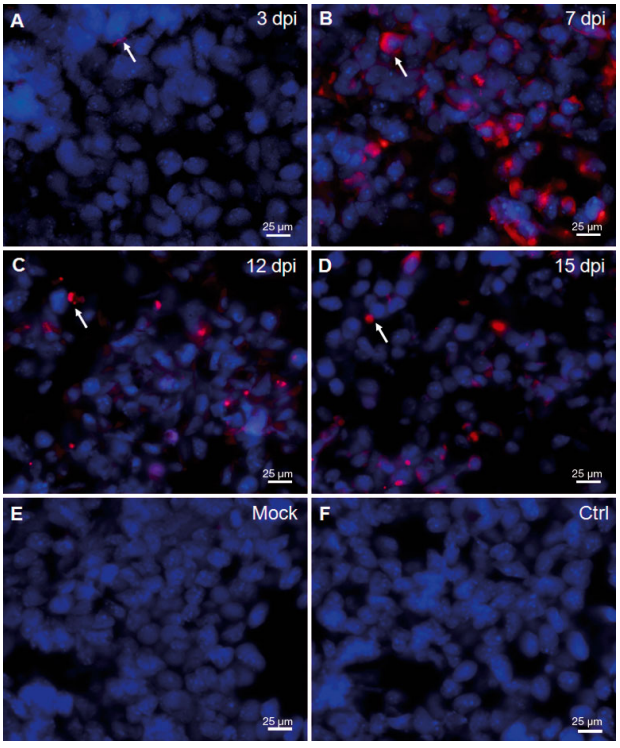


Fig. 6. *Andrias davidianus*. Fluorescent staining of tissue sections with a monoclonal antibody made against GSIV in the spleen of infected Chinese giant salamanders. (A–D) Spleen sections were obtained at 3, 7, 12 and 15 dpi. (E) Mock-infected spleen section. (F) Ctrl: 15 dpi spleen stained with the secondary antibody alone. Sections were counterstained with DAPI. Arrows indicate red fluorescence indicative of viral antigen; blue fluorescence indicates the nuclei of cells. Scale bars = 25 µm

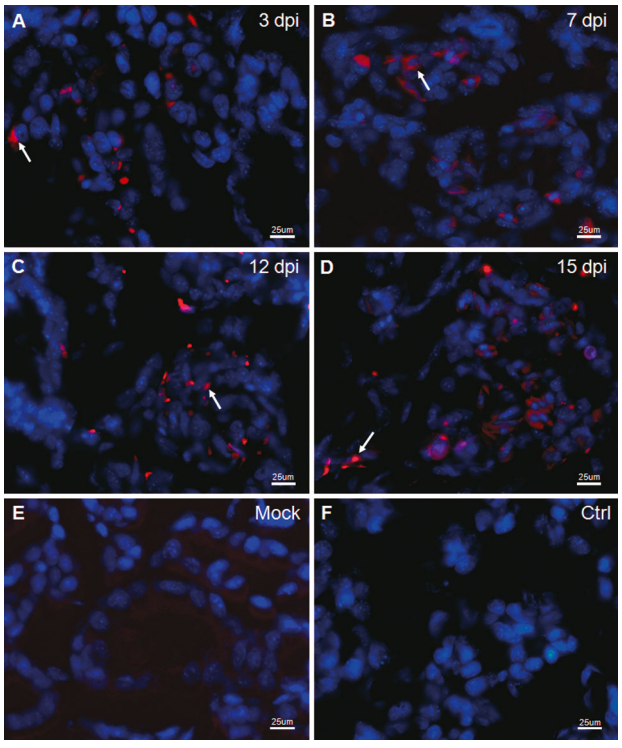


Fig. 7. *Andrias davidianus*. As in Fig. 6 for kidney sections

renal tubules, the glomerulus and hematopoietic tissues (Fig. 7A–D). In the liver, the percentage of GSIV antigen-positive cells increased from 3 to 7 dpi, and then decreased to a low level (Fig. 8A–D). In the gut, positive staining was not detected until 7 dpi, and then the prevalence increased slowly (Fig. 9A–D). No signal was detected in any mock-infected tissues (Figs. 6E, 7E, 8E & 9E). No signal was detected at 15 dpi in the infected tissues stained by the secondary antibody alone (Figs. 6F, 7F, 8F & 9F). In the heart and skin, no signal was observed (data not shown). The distribution of positive staining for the viral antigen is summarized in Table 3.

### Expression pattern of inflammation-related genes

Total RNA obtained from the different tissues mentioned above was examined for the expression of MIF, TNF-α and IL-1β. Using real-time PCR, RNA expression of MIF, TNF-α and IL-1β was found to be up-regulated at 3 dpi in the spleen. Compared to the expression level in the mock-infected group, the transcription of MIF and IL-1β in the spleen was increased about 59-fold and 79-fold, respectively (Fig. 10). TNF-α gene expression was increased about 4-fold at 7 dpi. The expression of these pro-inflammatory genes decreased in the spleen after 3 dpi. In the kidney, the expression of MIF increased 2.22-fold at 12 dpi. Additionally, the expression of TNF-α and IL-1β increased 6.59-fold and 10.34-fold, respectively, at 15 dpi. In the liver, at 7 dpi, the ex-

Table 3. *Andrias davidianus*. Mean ±SD percentage of GSIV antigen-positive cells in tissue sections prepared from the spleen, kidney, liver and gut of Chinese giant salamanders that were experimentally infected with GSIV. The number of positive cells and total cells (>100 cells) in 5 areas of 1 section were counted; 20 continuous sections of each tissue from 8 animals were measured

| Days post-infection | Spleen (%) | Kidney (%) | Liver (%) | Gut (%) |
|---|---|---|---|---|
| 3 | 1.5 ± 0.2 | 13.4 ± 4.5 | 2.1 ± 0.3 | 0 |
| 7 | 69.6 ± 6.7 | 24.8 ± 3.1 | 15.2 ± 2.2 | 2.6 ± 0.3 |
| 12 | 41.2 ± 4.3 | 53.8 ± 4.2 | 13.4 ± 1.8 | 8.4 ± 1.1 |
| 15 | 44.6 ± 3.8 | 56.2 ± 4.3 | 13.8 ± 2.0 | 8.1 ± 1.0 |

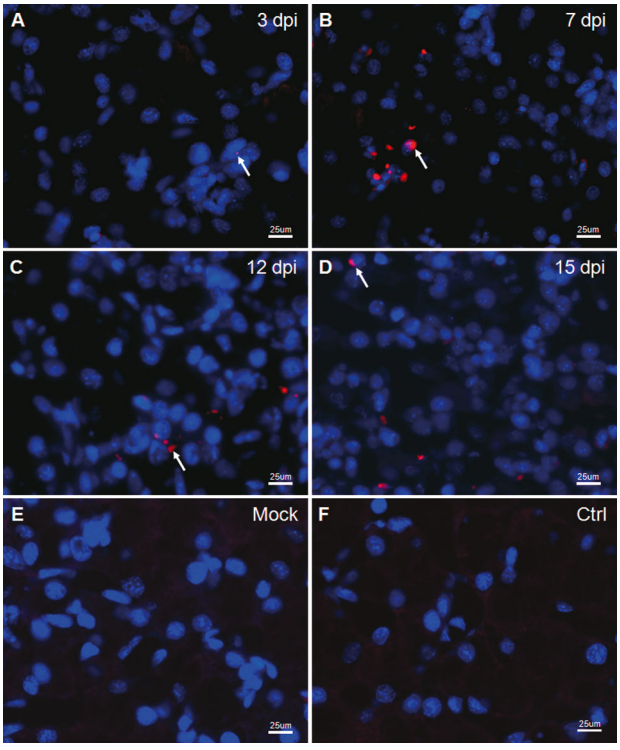


Fig. 8. *Andrias davidianus*. As in Fig. 6 for liver sections

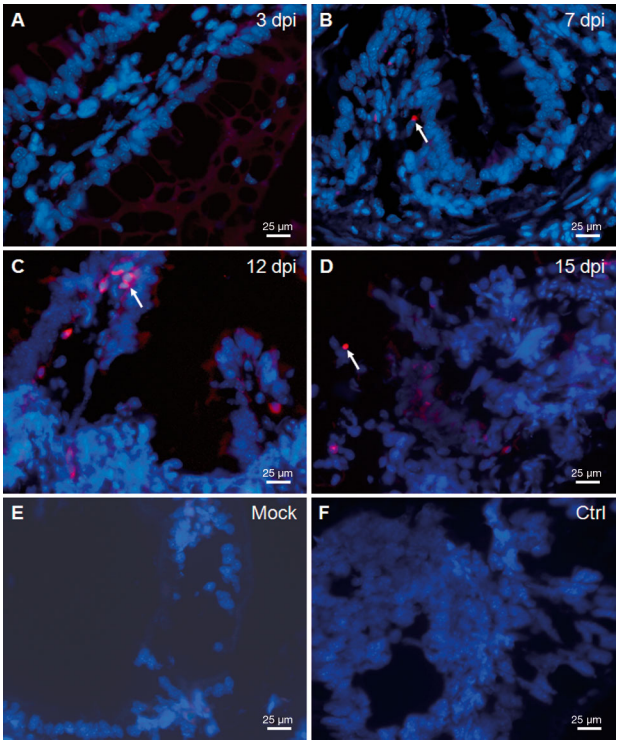


Fig. 9. *Andrias davidianus*. As in Fig. 6 for gut sections

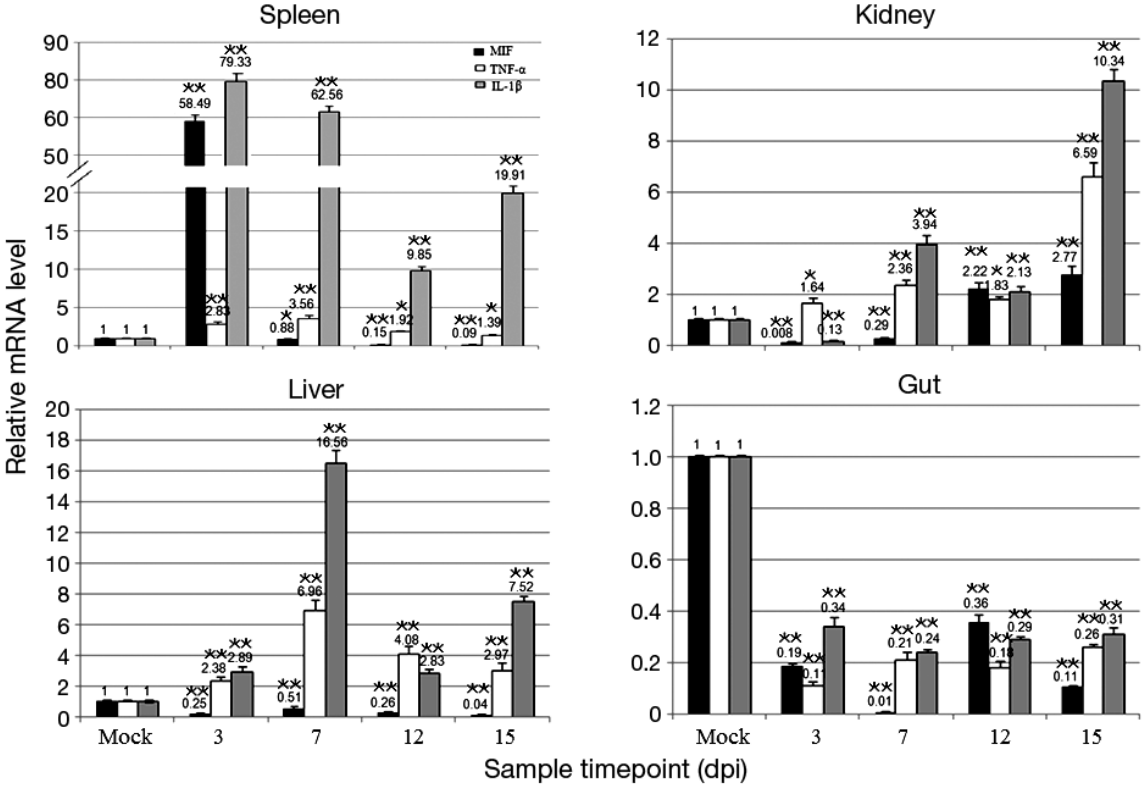


Fig. 10. *Andrias davidianus*. Quantitative real-time PCR analysis of MIF, TNF-α and IL-1β transcription levels in the spleen, kidney, liver and gut. The expression levels of each gene were normalized to 18S ribosomal RNA transcript levels and expressed in comparison to the mock infection group as a fold increase/decrease. $^{*}p \leq 0.05$; $^{**}p \leq 0.01$

pression of TNF-α and IL-1β was up-regulated 6.96-fold and 16.56-fold, respectively. However, the expression of MIF was significantly down-regulated compared to the mock-infected group. In the gut, the expression of MIF, TNF-α and IL-1β were all significantly down-regulated compared to the mock-infected group (Fig. 10).

## DISCUSSION

GSIV, a newly emerged infectious viral pathogen, causes high mortality and leads to huge economic losses. Viral inclusions were detected in spleen, kidney, liver and gut by hematoxylin and eosin staining (Dong et al. 2011, Geng et al. 2011, Chen et al. 2013, Meng et al. 2014). However, the tissue tropism of GSIV through the infection period is not well understood. In this study, the replication and distribution of the virus was investigated by IFA and *in situ* hybridization in different target organs. Replication and abundant GSIV antigen-positive cells were detected in the spleen, as observed with other ranavirus infections (Cunningham et al. 2008). Replication of GSIV increased dramatically in the spleen during the early stages of infection and then decreased, although the percentage of GSIV antigen-positive cells remained constant. In the kidney, there was a continuous increase in GSIV antigen-positive cells, which correlated with a high level of replication of the virus. A large number of GSIV antigen-positive cells was detected in the renal tubules, glomerulus and hematopoietic tissue which indicated that these cells may be susceptible to GSIV infection. The kidney was also shown to be susceptible to GSIV infection. GSIV was detected in the kidney until 15 dpi; however, the ranavirus frog virus 3 (FV3) can be cleared from the kidney of an infected frog at 9 dpi (Morales & Robert 2007). This suggests that the pathogenesis of GSIV is different from that of other ranaviruses. MCP-positive cells and GSIV antigen-positive cells were at a low prevalence in the liver, suggesting that the liver was not a major target organ of GSIV. In addition, less MCP expression/GSIV antigen was detected in both the mucosa epithelial cells and submucosa cells of the gut (Figs. 4A–D & 9A–D), which suggested that while the gut was susceptible to GSIV infection it was not a major target tissue.

GSIV induced a strong inflammatory response that increased expression of MIF, TNF-α and IL-1β. An indispensable inflammatory response mediator, MIF phosphorylates the ERK1/2, then activates cytosolic phospholipase $A_2$ and finally induces inflammatory response and increases production of inflammatory cytokines such as TNF-α (Flaster et al. 2007). MIF can also counter-regulate the inhibitory effects of glucocorticoids, which otherwise induce suppression of the inflammatory response (Calandra & Bucala 1997). TNF-α and IL-1β are common pro-inflammatory cytokines released from cells prior to the inflammation. Increased expression of TNF-α and IL-1β were reported in FV3-infected *Xenopus* and EPC cells and EHNV-infected EPC cells (Morales et al. 2010, Holopainen et al. 2012). In our study, GSIV infection triggered rapid and high expression of MIF, TNF-α and IL-1β in the spleen at 3 dpi, which may subsequently influence viral replication. This result demonstrates that inflammation plays a potential role in inhibition of virus replication in the immune organs of this amphibian. FV3 could induce rapid up-regulation of the inflammatory response in frogs (Morales et al. 2010) showing that ranaviruses could up-regulate inflammation in both a caudate and an anuran. However, the GSIV in the spleen of Chinese giant salamander was not cleared (Fig. 6A–D), indicating that inflammation might not contribute to virus clearance. Continued replication of virus in the kidney may be associated with a slowly induced inflammatory response, which could not reduce virus replication in damaged tissue during the later stages of infection. Replication of the virus in the liver and gut was not high, and the expression of MIF was down-regulated significantly in both tissues, although TNF-α and IL-1β expression increased slowly in the liver. This suggests that only a rapid and strong inflammatory response could inhibit virus replication. Our results demonstrated that GSIV infection initiates a strong inflammatory response in the spleen and a moderate inflammatory response in the kidney and liver. Rapid and strong inflammation could inhibit virus replication during the early stages of infection in some amphibian organs. The innate immune-related genes (MHC IA, IIA, IIB) were also up-regulated after GSIV infection (Zhu et al. 2014), especially in the spleen. Therefore, we believe that infection-elicited innate immune response(s) and inflammatory response(s) both play a critical role in conferring GSIV infection resistance to Chinese giant salamanders.

In conclusion, the results of this study demonstrate that the spleen and kidney were the major target tissues in the pathogenesis of GSIV, and their pro-inflammatory response plays a role in resistance against the replication of GSIV.

*Acknowledgements*. The work was supported by the Special Fund for Agro-Scientific Research in the Public Interest (201203086-05). We gratefully thank Dr. Scott E. LaPatra from Clear Springs Foods, Inc., Idaho, USA, for his help in revising and polishing this manuscript.

## LITERATURE CITED


- Balseiro A, Dalton KP, Del Cerro A, Marquez I, Parra F, Prieto JM, Casias R (2010) Outbreak of common midwife toad virus in alpine newts (*Mesotriton alpestris cyreni*) and common midwife toads (*Alytes obstetricans*) in northern Spain: comparative pathological study of an emerging ranavirus. Vet J 186:256–258
- Bernhagen J, Calandra T, Bucala R (1998) Regulation of the immune response by macrophage migration inhibitory factor: biological and structural features. J Mol Med 76:151–161
- Black PN, Blair CD, Butcher A, Capinera JL, Happ GM (1981) Biochemistry and ultrastructure of iridescent virus type 29. J Invertebr Pathol 38:12–21
- Calandra T, Bucala R (1997) Macrophage migration inhibitory factor (MIF): a glucocorticoid counter-regulator within the immune system. Crit Rev Immunol 17:77–88
- Calandra T, Roger T (2003) Macrophage migration inhibitory factor: a regulator of innate immunity. Nat Rev Immunol 3:791–800
- Calandra T, Bernhagen J, Metz CN, Spiegel LA and others (1995) MIF as a glucocorticoid-induced modulator of cytokine production. Nature 377:68–71
- Chen Z, Gui J, Gao X, Pei C, Hong Y, Zhang Q (2013) Genome architecture changes and major gene variations of *Andrias davidianus* ranavirus (ADRV). Vet Res 44:101
- Cunningham AA, Tems CA, Russell PH (2008) Immunohistochemical demonstration of ranavirus antigen in the tissues of infected frogs (*Rana temporaria*) with systemic hemorrhagic or cutaneous ulcerative disease. J Comp Pathol 138:3–11
- Das R, Koo MS, Kim BH, Jacob ST and others (2013) Macrophage migration inhibitory factor (MIF) is a critical mediator of the innate immune response to *Mycobacterium tuberculosis*. Proc Natl Acad Sci USA 110: E2997–E3006
- Dong W, Zhang X, Yang C, An J, Qin J, Song F, Zeng W (2011) Iridovirus infection in Chinese giant salamanders, China. Emerg Infect Dis 17:2388–2389
- Flaster H, Bernhagen J, Calandra T, Bucala R (2007) The macrophage migration inhibitory factor-glucocorticoid dyad: regulation of inflammation and immunity. Mol Endocrinol 21:1267–1280
- Geng Y, Wang KY, Zhou ZY, Li CW and others (2011) First report of a ranavirus associated with morbidity and mortality in farmed Chinese giant salamanders (*Andrias davidianus*). J Comp Pathol 145:95–102
- Holopainen R, Tapiovaara H, Honkanen J (2012) Expression analysis of immune response genes in fish epithelial cells following ranavirus infection. Fish Shellfish Immunol 32:1095–1105
- Hyatt AD, Gould AR, Zupanovic Z, Cunningham AA and others (2000) Comparative studies of piscine and amphibian iridoviruses. Arch Virol 145:301–331
- Jiang YL, Zhang M, Jing HL, Gao LY (2011) Isolation and characterization of an iridovirus from sick giant salamander (*Andrias davidianus*). Bing Du Xue Bao 27:274–282
- Jiang N, Jin X, He J, Yin Z (2012) The role of follisatin 1 in regulation of zebrafish fecundity and sexual differentiation. Biol Reprod 87:54
- Ma J, Zeng LB, Zhou Y, Jiang N, Zhang H, Fan Y, Meng Y, Xu J (2014) Ultrastructural morphogenesis of an amphibian iridovirus isolated from Chinese giant salamander (*Andrias davidianus*). J Comp Pathol 150:325–331
- Meng Y, Ma J, Jiang N, Zeng L, Xiao H (2014) Pathological and microbiological findings from mortality of the Chinese giant salamander (*Andrias davidianus*). Arch Virol 159:1403–1412
- Mitchell RA, Liao H, Chesney J, Fingerle-Rowson G, Baugh J, David J, Bucala R (2002) Macrophage migration inhibitory factor (MIF) sustains macrophage proinflammatory function by inhibiting p53: regulatory role in the innate immune response. Proc Natl Acad Sci USA 99:345–350
- Morales HD, Robert J (2007) Characterization of primary and memory CD8 T-cell responses against ranavirus (FV3) in *Xenopus laevis.* J Virol 81:2240–2248
- Morales HD, Abramowitz L, Gertz J, Sowa J, Vogel A, Robert J (2010) Innate immune responses and permissiveness to ranavirus infection of peritoneal leukocytes in the frog *Xenopus laevis.* J Virol 84:4912–4922
- Nishihira J (2000) Macrophage migration inhibitory factor (MIF): its essential role in the immune system and cell growth. J Interferon Cytokine Res 20:751–762
- Robert J, George E, De Jesús Andino F, Chen G (2011) Waterborne infectivity of the ranavirus frog virus 3 in *Xenopus laevis.* Virology 417:410–417
- Tidona CA, Schnitzler P, Kehm R, Darai G (1998) Is the major capsid protein of iridoviruses a suitable target for the study of viral evolution? Virus Genes 16:59–66
- Wang L, Yang H, Li F, Zhang Y, Yang Z, Li Y, Liu X (2013) Molecular characterization, tissue distribution and functional analysis of macrophage migration inhibitory factor protein (MIF) in Chinese giant salamanders *Andrias davidianus.* Dev Comp Immunol 39:161–168
- Wang XM, Zhang KJ, Wang ZH, Ding YZ, Wu W (2004) The decline of the Chinese giant salamander *Andrias davidianus* and implications for its conservation. Oryx 38: 197–202
- Yang L, Meng Z, Liu Y, Zhang Y and others (2010) Growth hormone and prolactin in *Andrias davidianus*: cDNA cloning, tissue distribution and phylogenetic analysis. Gen Comp Endocrinol 165:177–180
- Zhao Z, Teng Y, Liu H, Lin X, Wang K, Jiang Y, Chen H (2007) Characterization of a late gene encoding for MCP in soft-shelled turtle iridovirus. Virus Res 129:135–144
- Zhu R, Chen Z, Wang J, Yuan J, Liao X, Gui JF, Zhang QY (2014) Extensive diversification of MHC in Chinese giant salamanders *Andria davidianus* (Anda-MHC) reveals novel splice variants. Dev Comp Immunol 42:311–322


*Editorial responsibility: Louise Rollins-Smith, Nashville, Tennessee, USA*

*Submitted: September 23, 2014; Accepted: March 18, 2015*
*Proofs received from author(s): May 25, 2015*